MOMENTUM SPECTRA OF CHARGED HADRONS FROM THE DECAYS OF J/ψ AND ψ'

W. BRAUNSCHWEIG, H.-U. MARTYN, H.G. SANDER, D. SCHMITZ, W. STURM and W. WALLRAFF
I. Physikalisches Institut der RWTH Aachen, Germany

K. BERKELMAN[1], D. CORDS, R. FELST, E. GADERMANN, B. GITTELMAN[2], H. HULTSCHIG, P. JOOS, W. KOCH, U. KÖTZ, H. KREHBIEL, D. KREINICK, W.A. McNEELY, K.C. MOFFEIT, A. PETERSEN, B.H. WIIK and G. WOLF
Deutsches Elektronen-Syncrhtron DESY, Germany

G. GRINDHAMMER, J. LUDWIG, K.-H. MESS, G. POELZ, J. RINGEL, K. SAUERBERG and P. SCHMÜSER
II. Institut für Experimentalphysik der Universität Hamburg, Germany

W. De BOER, G. BUSCHHORN, B. GUNDERSON, R. KOTTHAUS, U.E. KRUSE[3], H. LIERL, H. OBERLACK, K. PRETZL and M. SCHLIWA
Max-Planck-Institut für Physik und Astrophysik, München, Germany

and

S. ORITO, T. SUDA, Y. TOTSUKA and S. YAMADA
University of Tokyo, Tokyo, Japan

Received 6 May 1976

Momentum spectra and particle ratios are presented for charged pions, kaons and nucleons emitted in the decays of J/ψ and ψ'.

In this paper we present the momentum spectra of charged pions, kaons and anti-protons observed in the decay of the J/ψ and ψ' resonances. The experiment was carried out at the DESY storage rings DORIS using the Double-Arm Spectrometer DASP.

A detailed description of DASP can be found in earlier publications [1]. It consists of two identical magnetic spectrometers symmetrically positioned with respect to the interaction point. Together the arms cover a geometrical solid angle of 0.9 sr. A non magnetic detector is located between the magnets. The trajectory of a charged particle is measured by two proportional chambers and a magnetostrictive chamber located before and by a set of six magnetostrictive chambers located behind the magnet. From the measured trajectory the momentum p of a particle is determined with a rms accuracy of $\Delta p/p = \pm 0.007\, p$ (GeV/c) with the magnet at $\frac{2}{3}$ of its full excitation leading to $\int B\, dl =$ 1.8 T·m. Since with this field the useful momentum acceptance begins at 0.45 GeV/c, 20% of the data were taken at a reduced field where the minimum accepted momentum was 0.15 GeV/c.

Particle identification is accomplished using information from the following detectors mounted behind the spark chambers:

a wall of scintillation counters located at an a distance of 4.7 m from the interaction point. Time-of-flight is measured between a small scintillation counter located at the beam pipe and this counter wall;

a set of lead scintillator shower counters each 6.2 radiation lengths thick;

a range counter hodoscope consisting of a 90 cm thick iron absorber subdivided into 5 sections with scintillation counters mounted behind 70 cm of iron.

In gathering these data we employed a pure inclusive trigger. The spectrometer was triggered when a single charged particle gave a signal in three scintillation counters before the magnet and in a time-of-flight

[1] Now at Cornell University, Ithaca, N.Y., USA.
[2] On leave from Cornell University, Ithaca, N.Y., USA
[3] Now at University of Illinois, Urbana, Ill., USA.

counter and a shower counter behind the magnet in one of the spectrometer arms. The trigger efficiency is thus independent of the final state and does not introduce any systematic uncertainties between pions, kaons and protons. The minimum momentum to trigger the detector (defined by the shower counter thresholds) was 0.14 GeV/c for a pion, 0.28 GeV/c for a kaon and 0.45 GeV/c for a proton (antiproton).

We scanned frequently with the beam energy in the mass region of the resonances. The energy was monitored by an NMR probe placed inside a ring bending magnet powered in series with the bending magnets in the rings. As a check the multihadron production was measured in the non magnetic detector while the inclusive spectra were being taken. This method is sensitive to energy shifts smaller than 0.2 MeV for energies near the resonance mass. The luminosity was determined by observing Bhabha scatters at a mean scattering angle of 8° using four identical scintillation-shower counter hodoscopes. An absolute normalization was obtained by comparing the rates in these counters with the large angle Bhabha scattering observed in the inner detector at energies outside the resonances. The data reported here correspond to a total integrated luminosity of 185 nb^{-1} and 325 nb^{-1} for energies near the J/ψ and ψ' respectively.

The data so obtained were analyzed as follows:

The measured interaction volume is 4 cm long and less than 0.1 cm in diameter. Reconstructed tracks were required to originate within ±3.5 cm of the nominal interaction point measured along the beam direction and ± 1 cm measured in the vertical direction.

The first step in particle identification was to remove muon and Bhabha pair events from the data sample by using the collinearity, momentum, range counter and shower energy information.

Hadrons were identified by the time-of-flight measurement. The rms time resolution of ±0.26 ns and an average flight path of 5 m suffice to separate pions from kaons up to 1.5 GeV/c, and kaons from protons up to 3 GeV/c (ref. [2]). Fig. 1a shows the distribution of the square of the particle mass calculated from the velocity β and momentum $p, M^2 = (p/\beta)^2 (1-\beta^2)$, for several momentum intervals. Protons and antiprotons were uniquely identified by time-of-flight. Since a sizeable fraction of the protons came from beam gas interactions only antiprotons were used in the analysis. The proton yield was assumed to equal that of antiprotons.

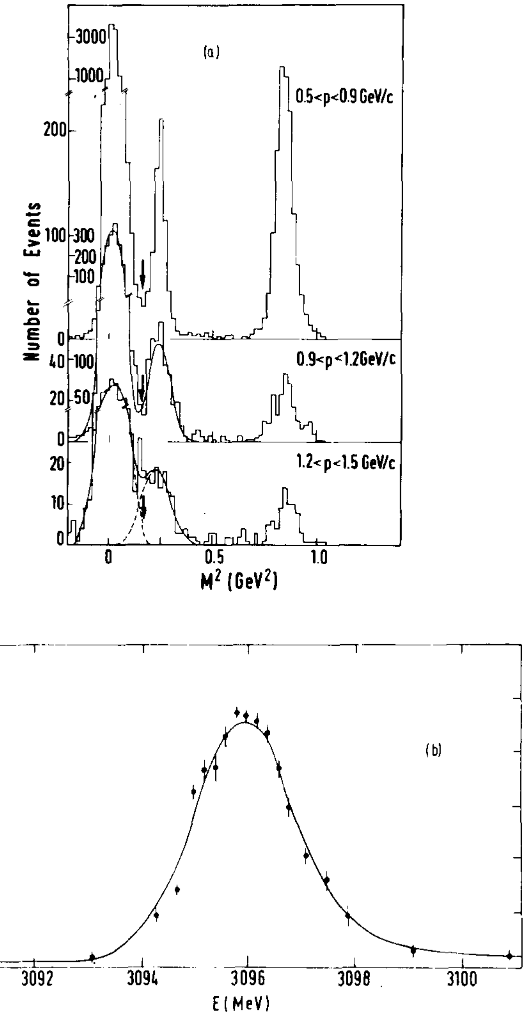

Fig. 1. (a) Histograms of mass squared as computed from particle momentum and time-of-flight for several momentum intervals. (b) Cross section for inclusive hadron production, $e^+e^- \to h^\pm X$, at the J/ψ resonance as a function of the total cms energy integrated over particle momenta between 0.5 and 1.3 GeV/c. The curve is the result of a fit described in the text.

From the remaining data sample, all tracks for which a range counter had fired were identified as muons.

The arrows shown in fig. 1a mark the cut used to separate pions from kaons. In the highest momentum interval (1.2 to 1.5 GeV/c) a fit was made to determine the pion and kaon fractions. The pion contamination of the kaon signal and the kaon contamination of the pion signal were found to be less than 5%; approximately 20% of the kaons were lost due to the cut. The data were corrected accordingly.

Additional pulse height cuts were made to eliminate electrons. Pions (kaons) were required to have a pulse height less than 5 times (10 times) that of a minimum ionizing particle.

Pions from K^0 decay and antiprotons from hyperon decay were included.

A total of 18,000 $\pi^\pm$, 1500 $K^\pm$ and 560 antiprotons were obtained at the J/ψ. The corresponding numbers for the ψ' were 7000 $\pi^\pm$, 600 $K^\pm$, and 200 antiprotons.

To convert particle counts into cross sections requires knowledge of the experimental acceptance and of various correction factors. To avoid uncertainties near the acceptance boundary only events within a restricted acceptance (typically smaller 30% than the actual one) were used. A comparison of the cross sections determined for the full and the restricted acceptances did not reveal any statistically significant differences, however. The restricted acceptance covered typically polar angles between $\cos\theta = -0.55$ and 0.55. Each observed particle's track was weighted to account for limited acceptance and detection inefficiencies:

(1) The angular distributions were found to be consistent with isotropy over the polar angles accepted. Except for $\pi\rho$ and KK^* events an isotropic angular distribution was assumed to extrapolate to the full solid angle. This introduced systematic uncertainties (not shown in the figures) which are typically < 10% for $p < 1$ GeV/c and < 20% for $p > 1$ GeV/c. For $\pi(K)$ recoiling against a $\rho(K^*)$ missing mass a $(1 + \cos^2\theta)$ angular dependence was taken.

(2) Correction factors for nuclear absorption were applied. They were typically 1.035 and 1.21 for 0.5 GeV/c pions and antiprotons, respectively.

(3) Between 0.15 and 1.3 GeV/c 42% to 6% of the pions decay before the shower counter. Of the kaons 71% to 38% decay for momenta between 0.5 and 1.3 GeV/c. However, decaying pions and kaons have a momentum dependent probability to be accepted by the track finding programs. A Monte Carlo analysis was used to correct the data accordingly.

(4) The correction factor for tracks failing reconstruction was 1.15.

(5) The correction factor for loss of tracks due to electronic failure was 1.08.

Events from beam gas interactions must be accounted for by a subtraction. This background was found to be uniformly distributed along the beam axis over a distance of ±15 cm with respect to the center of the interaction region. The beam gas rate was extrapolated into the interaction region. The subtraction was done separately for each momentum interval and each particle species. At the J/ψ the beam gas background contributed 3% of the signal for momenta less than 0.5 GeV/c and 0.5% above. The corresponding numbers at the ψ' were 17% and 4%. The background from cosmic ray interactions was found to be negligible.

The uncertainty in these corrections lead to an overall normalization uncertainty of ±15%.

The excitation curves were used to integrate cross sections over the resonance. Fig. 1b shows the cross section for production of charged hadrons with momenta between 0.5 and 1.3 GeV/c in the region of the J/ψ resonance. The observed shape of the resonance is determined by the spread in beam energy (σ_{beam} = 0.6 MeV at 1.5 GeV) and radiative effects. The theoretical curve [3,4] was fitted to the data treating the resonance mass, the beam energy spread and the resonance contribution as free parameters*. The resulting resonance contribution was integrated over the total cms energy E and corrections were made for radiative effects in the initial state. For integration of the resonance contribution up to 3100 MeV the radiative correction factor was 1.39. The weighted data were finally normalized to the integrated cross section. This procedure was done separately for each magnet setting. The cross sections given below represent energy integrals over the resonance contributions, e.g. $d\sigma/dp$ stands for $\int_R d\sigma(E)/dp\, dE$.

Figs. 2a, b show the momentum spectra for $\pi^\pm$ (i.e. sum of π^+ and π^-), $K^\pm$ and $2\bar{p}$ from J/ψ and ψ' decay. The error bars do not reflect the ±15% normalization uncertainty. The π^+ and $\pi^-(K^+, K^-)$ yields were found to be equal to within 3% (2%). Both resonances show qualitatively the same behaviour. The pion and kaon yields decrease approximately exponentially with increasing momentum, but with different slopes. At 0.5 GeV/c the K yield is a factor of ~10 below the pion yield but approaches the pion yield with increasing momentum. The double $\bar{p}$ yield is a factor of two below the K cross section. For the J/ψ we observe the $\pi^\pm\rho^\mp$ and $K^\pm K^{*\mp}$ decay channels as enhancements near the kinematical limit. The structures in the $\bar{p}$ yield

* The fitted resonance masses were 3096 MeV and 3687 MeV. These values differ by 0.18% from our previously published values due to a careful recalibration of the storage ring orbits [5].

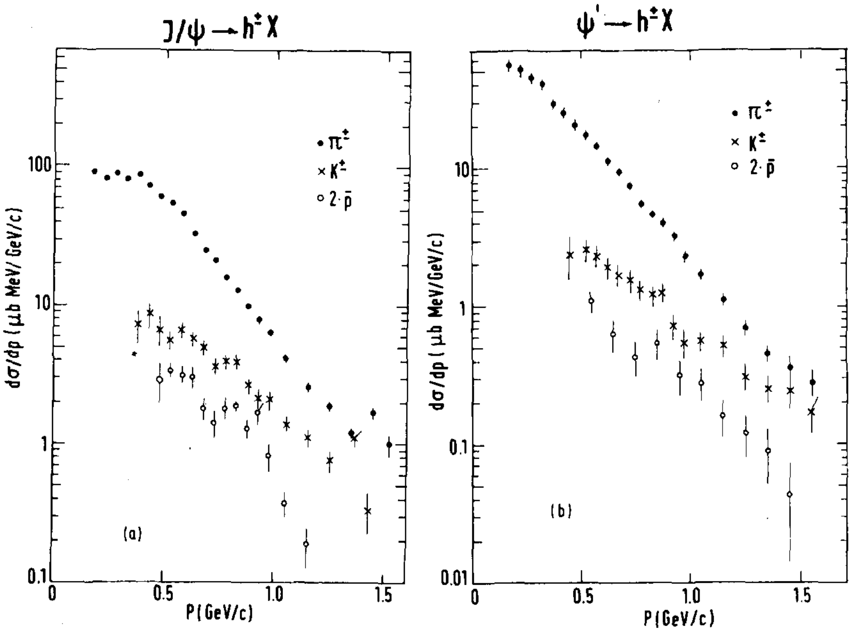

Fig. 2. Differential cross sections, $d\sigma/dp$, for $\pi^\pm$, $K^\pm$ and $\bar{p}$ for the J/ψ and ψ' integrated over the resonance as described in the text. The $\bar{p}$ yield has been multiplied by a factor of two.

might be a reflection of N*(1520) and N*(1688) production.

The particle ratios, e.g. R_π = (number of $\pi^\pm$)/(sum of $\pi^\pm$, $K^\pm$ and $2\bar{p}$) are plotted as a function of momentum in fig. 3. At $p = 1.3$ GeV/c nearly 30% of all charged particles produced are kaons while protons and antiprotons account for roughly 10%. We determined the particle ratios averaged over all momenta. The invariant cross sections $E/4\pi p^2 \, d\sigma/dp$ were fitted to a simple exponential (see below) in order to extrapolate the particle yields to zero momentum. The result is

$$J/\psi: \quad R_{\pi^\pm} = 87.5 \pm 1.3\% , \quad R_{K^\pm} = 8.9 \pm 1.0\% , \quad R_{p,\bar{p}} = 3.6 \pm 0.9\% ,$$

$$\psi': \quad R_{\pi^\pm} = 90.8 \pm 1.0\% , \quad R_{K^\pm} = 6.9 \pm 0.9\% , \quad R_{p,\bar{p}} = 2.3 \pm 0.7\% .$$

No significant difference between J/ψ and ψ' is observed; in particular the K fraction for the ψ' is not larger than for the J/ψ. 57±8% (ref. [6]) of the ψ' decay proceeds via the cascade channel $\psi' \to J/\psi' X$. The particle ratios from the remaining decay channels can be evaluated by subtracting off the cascade contribution from J/ψ decay and from $X = \pi^+\pi^-$, and $X = \eta$. Within errors, the resulting ratios

$$\psi' \text{ (not decaying via } J/\psi): \quad R_{\pi^\pm} = 90.0 \pm 3\% , \quad R_{K^\pm} = 8.5 \pm 2.7\% , \quad R_{p,\bar{p}} = 1.5 \pm 1.9\% ,$$

are the same as for the J/ψ and the total ψ' decays.

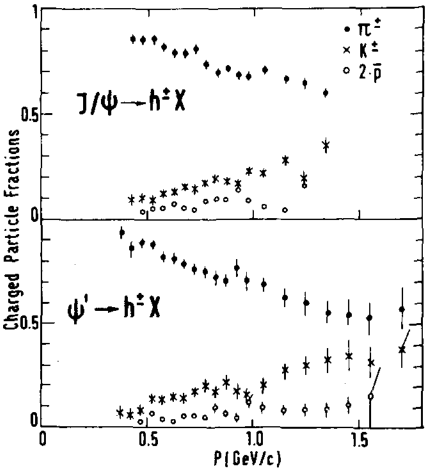

Fig. 3. Charge λ particle fractions as a function of momentum for the J/ψ and ψ'. The $\bar{p}$ fraction has been multiplied by a factor of two.

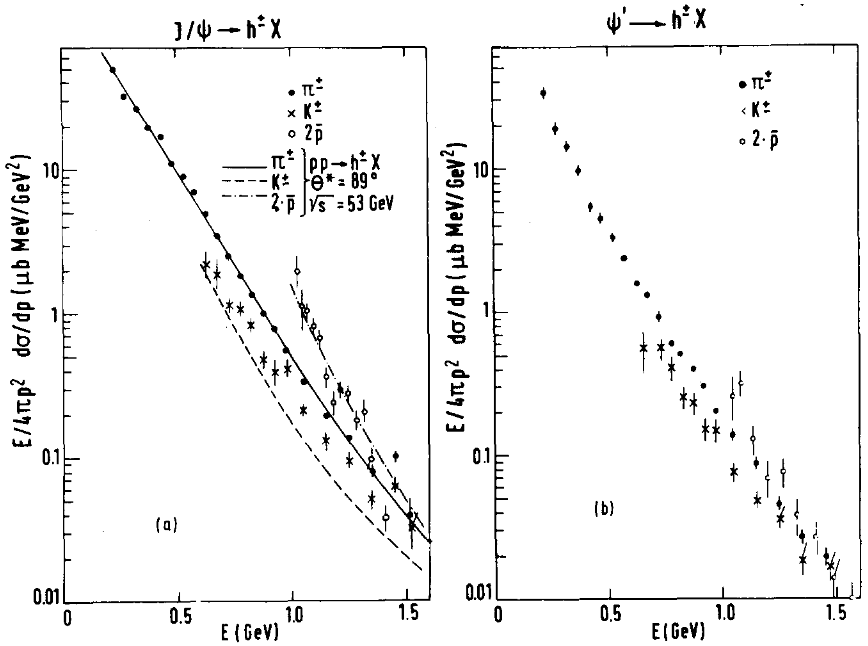

Fig. 4. Invariant cross sections, $E/4\pi p^2\, d\sigma/dp$, integrated over the resonance for $\pi^\pm$, $K^\pm$ and $\bar{p}$ for the J/ψ and ψ'. The $\bar{p}$ cross section has been multiplied by a factor of two. The curves in fig. 4a describe the inclusive particle yields from $pp \to h^\pm X$ (ref. [7]).

In fig. 4 we present the invariant cross sections $E/4\pi p^2\, d\sigma/dp$ as a function of particle energy. The pion yield from the J/ψ can be described by a single exponential. For the ψ' we observe a break around $E_\pi = 0.4$ GeV. The excess of events for $E_\pi < 0.4$ GeV is due to the $\pi^\pm$ emitted in the cascade decay $\psi' \to \pi^+\pi^- J/\psi$. For both J/ψ and ψ' the $K^\pm$ yield is a factor of 1.5–2 below the $\pi^\pm$ yield; the $2\bar{p}$ yield lies above the $\pi^\pm$ cross section by about the same factor. Fits to the data of the form $\exp(-bE)$ lead to the following values for b in GeV^{-1}:

$$J/\psi:\quad b_\pi = 5.9\pm0.1\,,\quad b_K = 5.2\pm0.3\,,\quad b_{\bar{p}} = 7.2\pm0.6\,,$$

$$\psi':\quad b_\pi = 5.8\pm0.1\ (\text{for } E_\pi > 0.5\ \text{GeV})\,;$$

$$b_k = 4.7\pm0.3\,,\quad b_{\bar{p}} = 6.3\pm0.6\,.$$

In a thermodynamical description the observed slopes correspond to a temperature of about 170 MeV. The broad features we observe in the invariant cross sections are surprisingly similar to those for pp collisions at ISR energies in the central region [7, 8] when $E/4\pi p^2\, d\sigma/dp$ is plotted as a function of the transverse energy $E_T \equiv \sqrt{p_\perp^2 + m^2}$ instead of E. This is demonstrated for the J/ψ by the curves in fig. 4 which were taken from Alper et al. [7] employing one overall normalization factor. We observe relative to $\pi^\pm$ production somewhat more kaons than in the pp data.

We thank all engineers and technicians of the collaborating institutions who have participated in the construction of DASP. The invaluable cooperation with the technical support groups and the computer center at DESY is gratefully acknowledged. We are indebted to the DORIS machine group for their excellent support during the experiment. The non-DESY members of the collaboration thank the DESY Direktorium for the kind hospitality extended to them.

References

[1] DASP collaboration, Phys. Letters 53B (1974) 393; 53B (1975) 491; 56B (1975) 491; 57B (1975) 297; 57B (1975) 467.

[2] W. Braunschweig, E. Könings, W. Sturm and W. Wallraff, Univ. of Aachen preprint HEP 75/11 (1975); and Nucl. Instr. Methods, to be published.

[3] J.D. Jackson and D. Scharre, Nucl. Instr. Methods 128 (1975) 13.
[4] D.R. Yennie, Phys. Rev. Letters 34 (1975) 239; F.A. Berends and N. Komen, private communication.
[5] H. Degele, private communication.
[6] G.S. Abrams et al., Phys. Rev. Letters 34 (1975) 481.
[7] British-Scandinavian Collaboration, B. Alper et al., Nucl. Phys. B87 (1975) 19.
[8] J. Engels, H. Satz and K. Schilling, Nuovo Cimento 17A (1973) 535; F. Elvekjiar, and F. Steiner, Phys. Letters 60B (1976) 456; F. Elvekjiar, DESY report 75/53 (1975).